Supplementary figure 1:

Protein score distribution obtained in mass spectrometry analysis of immunoprecipitation experiments

Protein log2 score distributions obtained in a typical immunoprecipitation experiment were compared between control (no tagged BY4741) and Tma108-PA samples. Most proteins (53%) were detected only in Tma108-PA, their score are artificially set to 1 in BY4741 IP: they correspond to the peaks observed in BY4741 distribution. According to the distribution of BY4741 IPs, a threshold value of log2 (8 in this example) was chosen in order to distinguish specifically interacting proteins from the background. Moreover, we kept only proteins whose ratio between Tma108-PA and BY4741 IP was superior to 2. Finally, only proteins reproducibly detected in replicate experiments were kept in the final list.

TMA108-PA IP

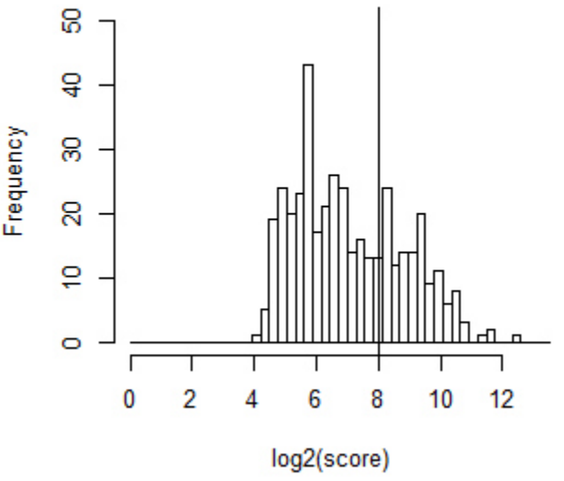

BY4741 IP

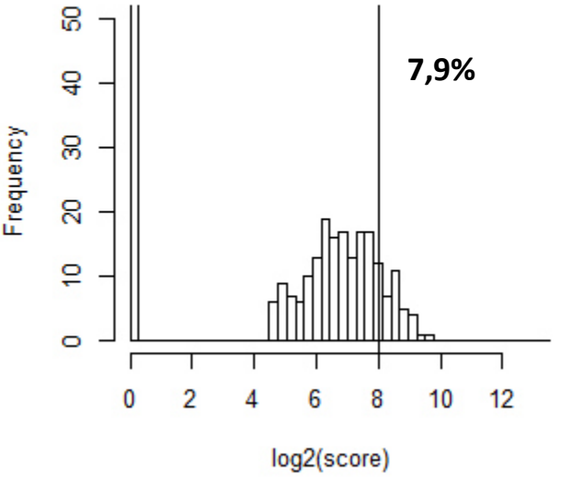

Supplementary figure 2:

Phylogenic tree showing Tma108, Aap1 et Ape2 orthologues in *Saccharomycetaceae.*

Homologues of *S. cerevisiae* Tma108, Aap1 and Ape2 were searched in the sequenced genomes of *Saccharomycetaceae*. After multiple alignments of the retrieved sequences, a phylogenic tree showing evolutionary distances between the different proteins was built. On this tree, only the 18 Tma108 sequences used for the conservation analysis are shown. Tma108 sequences (red background) belong to a distinct branch from Aap1/Ape2 homologues (green background). The species are indicated in brackets. The arrow indicates *S. cerevisiae* sequences. Accession numbers are available in table S4.

Delaveau et al. Fig. S2

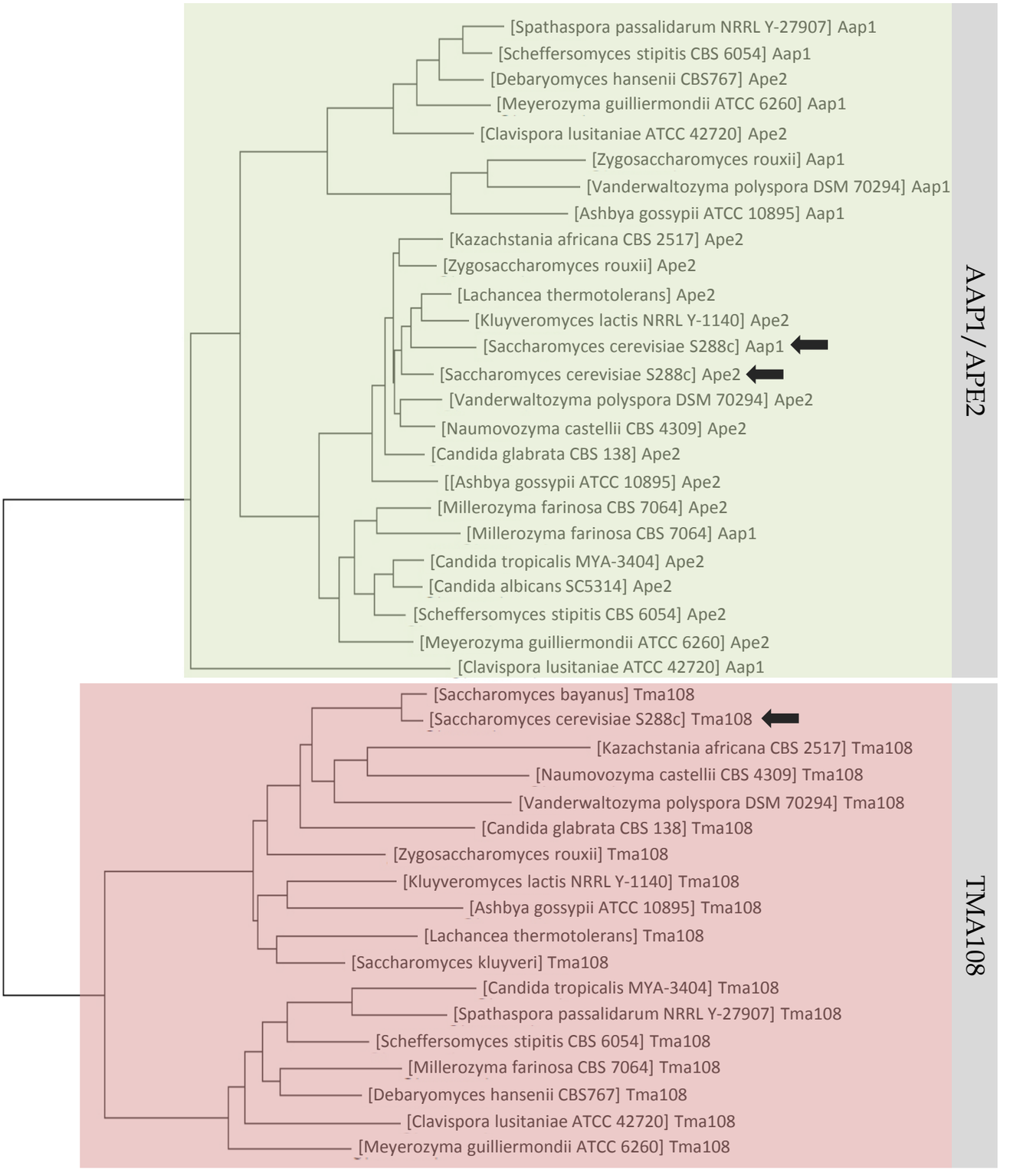

Supplementary figure 3:

Tma108 positioning in a phylogenic tree of M1 aminopeptidases

The sequences of 14 well-characterized M1 aminopeptidases (11 *Homo sapiens*, 1 *E.coli*, 2 *S. cerevisiae* sequences) were used for multiple alignment with ScTma108. The result was used to build a phylogenic tree showing evolutionary distances between the different proteins. For each protein, the specie and the percentage of identity with Tma108 sequence is indicated in brackets. The protein used for the alignment are (species are indicate in brackets; accession number are available in Table S4): TMA108 [Saccharomyces cerevisiae];APE2, Aminopeptidase yscII [Saccharomyces cerevisiae]; AAP1, Arginine/alanine amino peptidase [Saccharomyces cerevisiae]; PSA, puromycin-sensitive aminopeptidase [Homo sapiens]; AP-Q, aminopeptidase Q [Homo sapiens]; Ap-N, aminopeptidase N [Homo sapiens]; TRH-DE, thyrotropin-releasing hormone degrading enzyme [Homo sapiens]; Ap-A, aminopeptidase A [Homo sapiens]; ERAP1 , endoplasmic reticulum aminopeptidase 1 [Homo sapiens] ; ERAP2, endoplasmic reticulum aminopeptidase 2 [Homo sapiens]; IRAP, oxytocinase/insulin-responsive aminopeptidase [Homo sapiens]; ePepN, E. coli Aminopeptidase N [Escherichia coli]; LTA4H, Human Leukotriene A4 Hydrolase [Homo sapiens]; Ap-B, aminopeptidase B [Homo sapiens]; RNPEP-L1, arginyl aminopeptidase-like 1 [Homo sapiens].

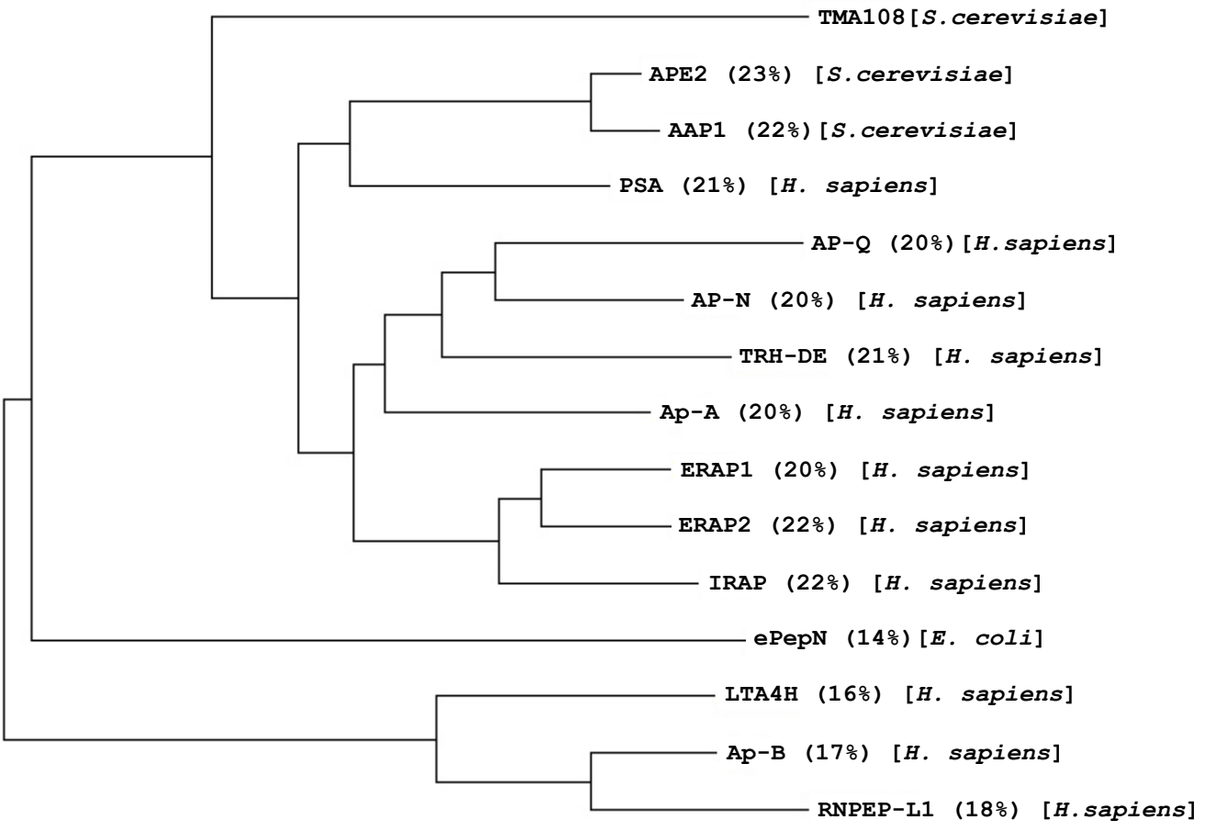
TMA108[S.cerevisiae]
APE2 (23%) [S.cerevisiae]
AAP1 (22%)[S.cerevisiae]
PSA (21%) [H. sapiens]
AP-Q (20%)[H.sapiens]
AP-N (20%) [H. sapiens]
TRH-DE (21%) [H. sapiens]
Ap-A (20%) [H. sapiens]
ERAP1 (20%) [H. sapiens]
ERAP2 (22%) [H. sapiens]
IRAP (22%) [H. sapiens]
ePepN (14%)[E. coli]
LTA4H (16%) [H. sapiens]
Ap-B (17%) [H. sapiens]
RNPEP-L1 (18%) [H.sapiens]

Supplementary figure 4:

Hypothesis to explain the impact of Tma108 on *ATP2* mRNA localization to mitochondria

(a) Current model of *ATP2* mRNA targeting to mitochondria. Previous studies demonstrated that *ATP2* mRNA localization is a co-translationnal process mediated by the interaction of the native MTS (Mitochondrial Targeting Sequence) with the mitochondria surface {Garcia, 2010 #70} {Eliyahu, 2010 #86}. The association of the translating complex with the mitochondria surface is dependent upon the translation speed: the elongation might be slow enough to keep the interaction of the ribosome with the mRNA.

(b) Two hypotheses that could explain Tma108 negative impact on *ATP2* mRNA localization. (1) The interaction of Tma108 with the nascent-chain could reduce the ability of the MTS to interact with the mitochondria. (2) Tma108 could increase the speed of *ATP2* translation impairing the co-transitional addressing of *ATP2* mRNA along with the nascent chain by a premature release of the translation machinery.

a: Mechanism of co-translational localization of *ATP2* mRNA

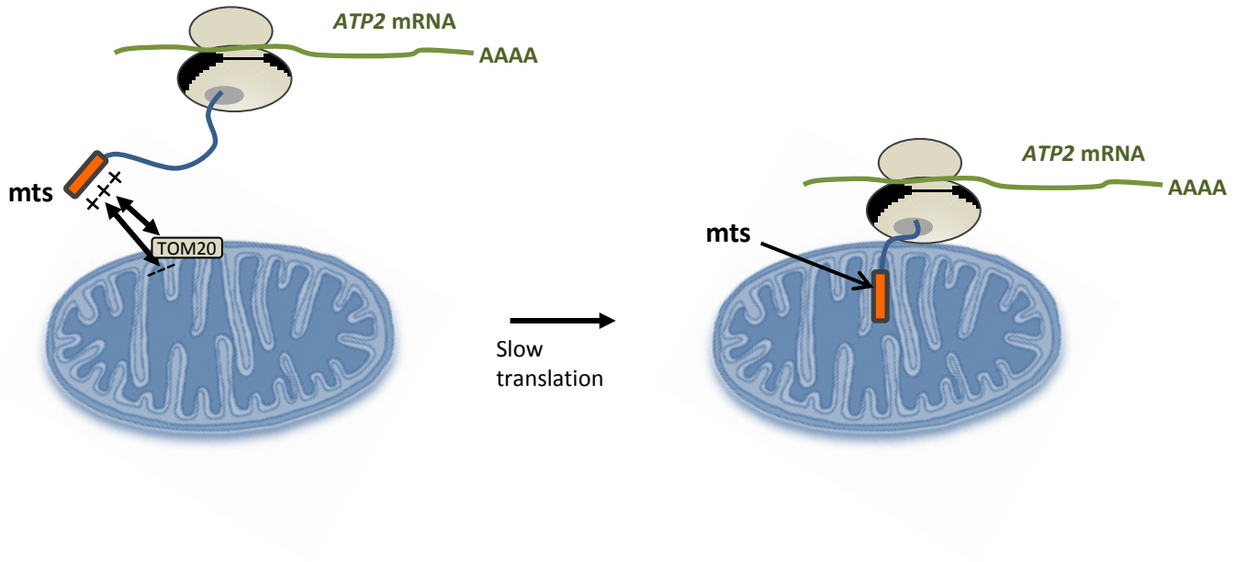

b:TMA108 negative impact on ATP2 mRNA localization:

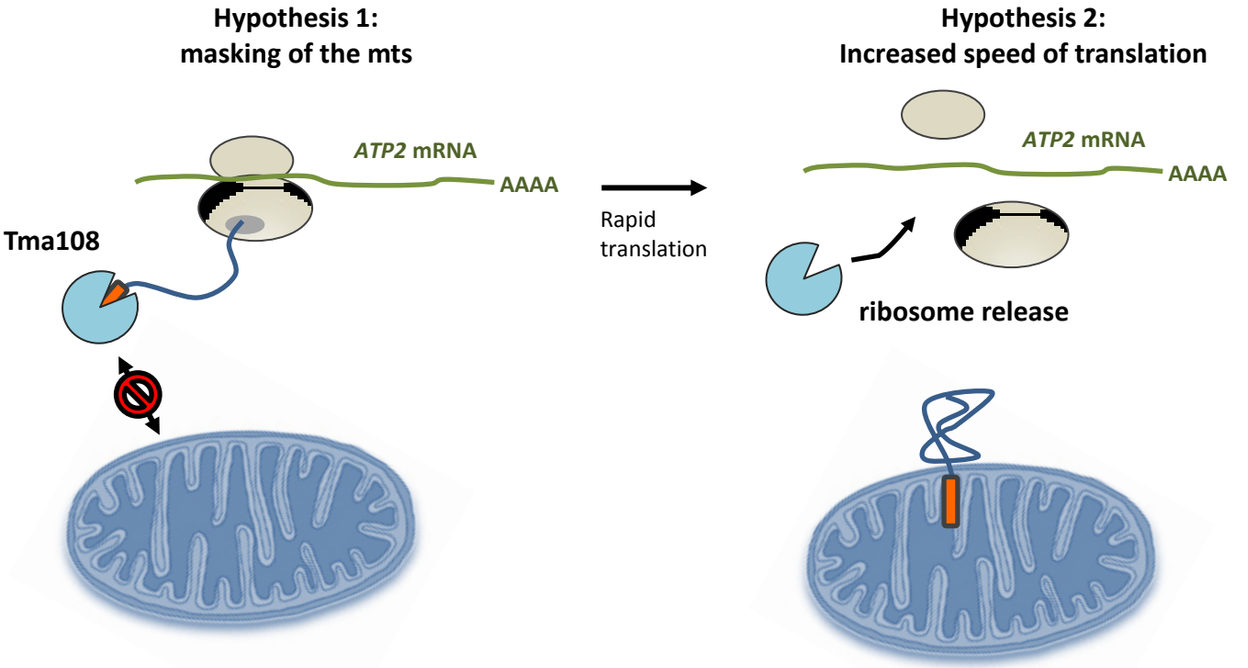

Supplementary figure 5:

***ATP2* mRNA localization phenotype and functional complementation of Tma108 deletion**

(a) *ATP2* mRNA localization to mitochondria was analyzed by quantitative FISH, as described in figure 1A, in *TMA108+/+* (BY4743), *tma108Δ/TMA108+* or *tma108Δ/Δ* cells and *tma108Δ/Δ* cells transformed with a pTMA108 plasmid. This plasmid encompasses the complete *TMA108* coding sequence under the control of its cognate promotor and terminator. The hyperlocalization phenotype of *ATP2* mRNA observed in *tma108Δ/Δ* cells is partially reverted in *tma108Δ/TMA108+* and in *tma108Δ/Δ* +pTMA108 cells.

(b) Analysis of *TMA108* mRNA levels by Q-PCR. Ratios from two replicates are obtained following normalization to *ACT1* mRNA levels. As expected, *TMA108* was not detected (ND) in *tma108Δ/Δ* cells. *tma108Δ/TMA108+* and in *tma108Δ/Δ* +pTMA108 cells showed a reduced level of *TMA108* mRNA, as compared to the wild type BY4743 strain, that correlated with the ATP2 localization phenotype scored in A. Note that the higher intercellular heterogeneity observed for ATP2 localization in *tma108Δ/Δ* +pTMA108 cells might be caused by variable copy numbers of the pTMA108 plasmid.

a

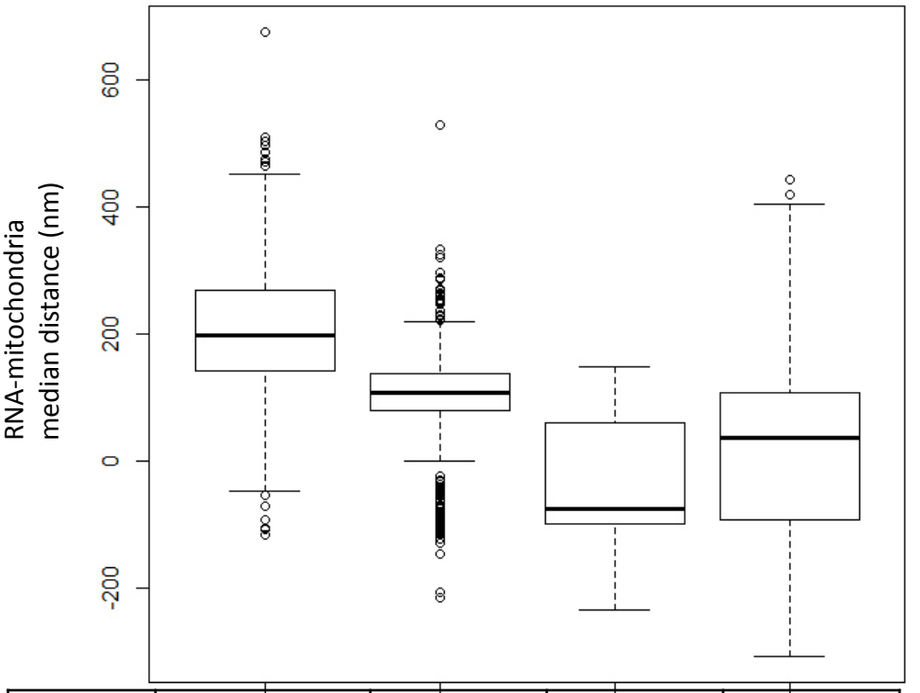

Strain	BY4743	*tma108Δ/* TMA108+	*tma108Δ/Δ*	*tma108Δ/Δ*
Plasmid	/	/	/	pTMA108

b

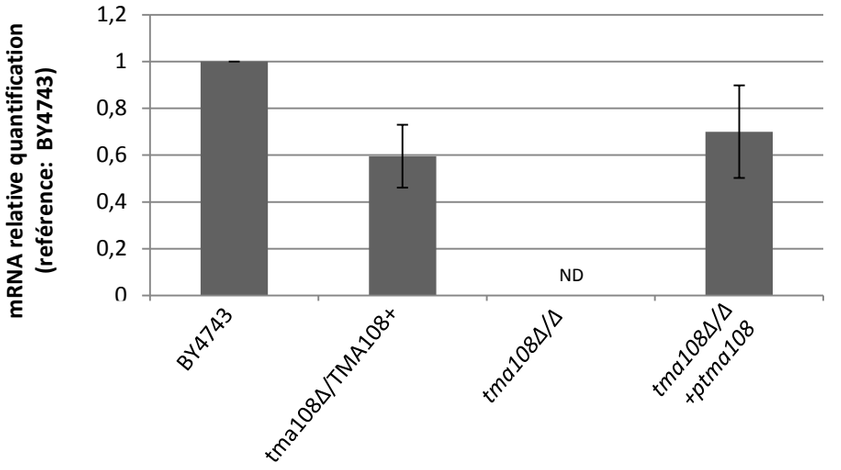

Supplementary figure 6:

Surexpression of Tma108 induces a delocalization of ATP2 mRNA

(a) Analysis of *ATP2* mRNA localization to mitochondria in BY4743 and *tma108Δ/Δ* cells transformed or not with the pGal-TMA108 plamid. This plasmid encompasses the complete coding sequence of *TMA108* under the control of the galactose-inducible *GAL1* promoter. A 13Myc tag was inserted in the C-terminus of Tma108 in order to control protein expression by immunobloting (C). The histograms show the distributions of *ATP2*-mitochondria median distances (d) in more than 200 hundred cells. The red lines delimitate 3 areas in the cellular population: cells with hyperlocalized *ATP2* (d<0), cells with intermediate phenotype of localization (0<d<300nm), cells with delocalized *ATP2* (d>300nm). The surexpression of Tma108 with pGal-TMA108 leads, both in BY4743 and *tma108Δ/Δ*, to a significant change of the distribution of cells within these 3 categories. In both cases, an increase of the number of cells with delocalized *ATP2* was observed. A decreased of the number of cells exhibiting the *ATP2* hyperlocalization phenotype was also recorded in TMA108-overexpressing *tma108Δ/Δ* cells.

(b) Real Time Q-PCR analysis of *TMA108* mRNA expression in *tma108Δ/Δ* + pGal-TMA108 cells (as compared to BY4743) .

(c) Immunodetection of Tma108 expressed from the pGal-Tma108 plasmid (1) of from a BY4742-derived strain containing a 13myc genomic tag at the C-terminus of TMA108 (2). Same amounts of protein extracts were analyzed by SDS-PAGE followed by anti-Myc western blot.

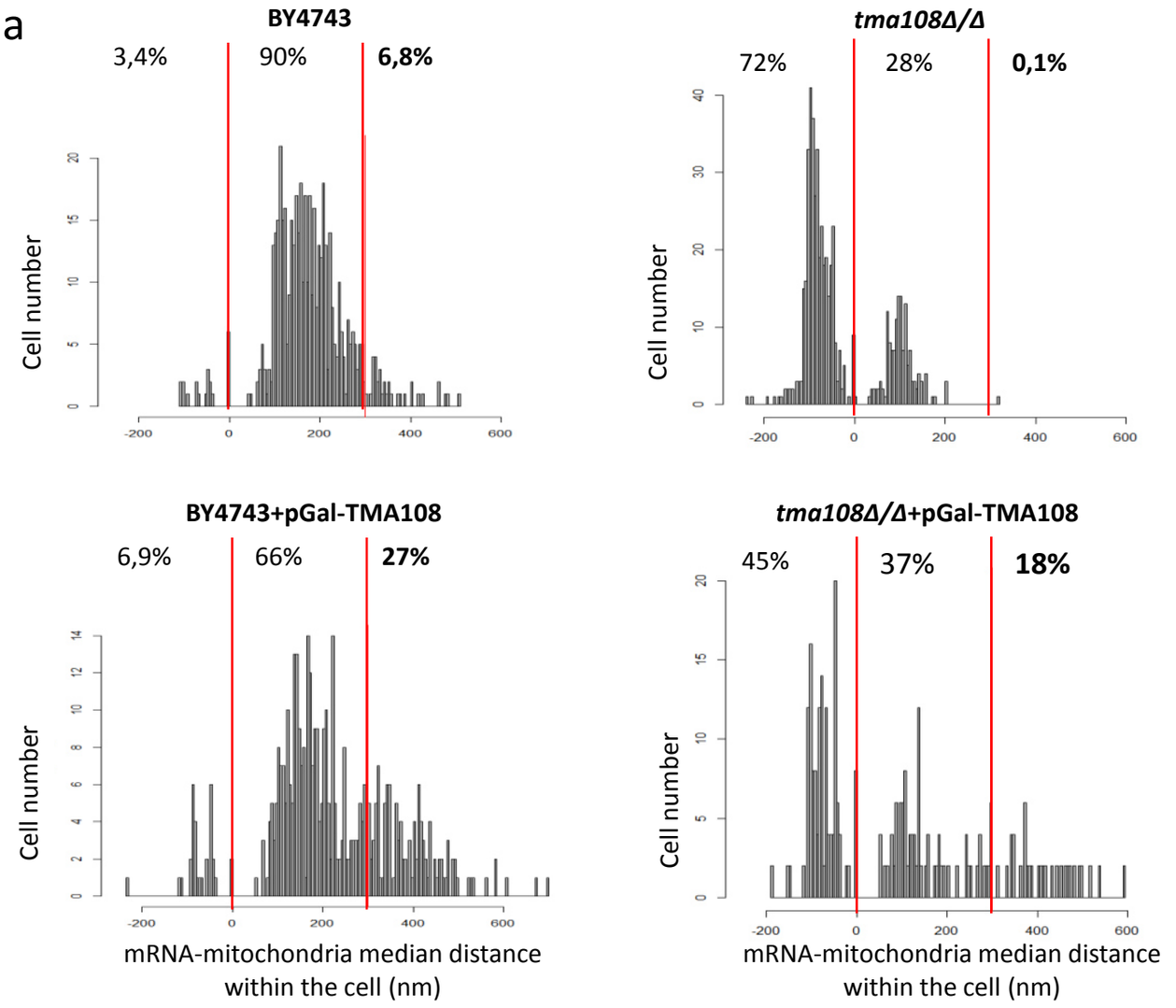
a
BY4743
3,4%
90%
6,8%
tma108Δ/Δ
72%
28%
0,1%
BY4743+pGal-TMA108
6,9%
66%
27%
tma108Δ/Δ+pGal-TMA108
45%
37%
18%
Cell number
mRNA-mitochondria median distance within the cell (nm)

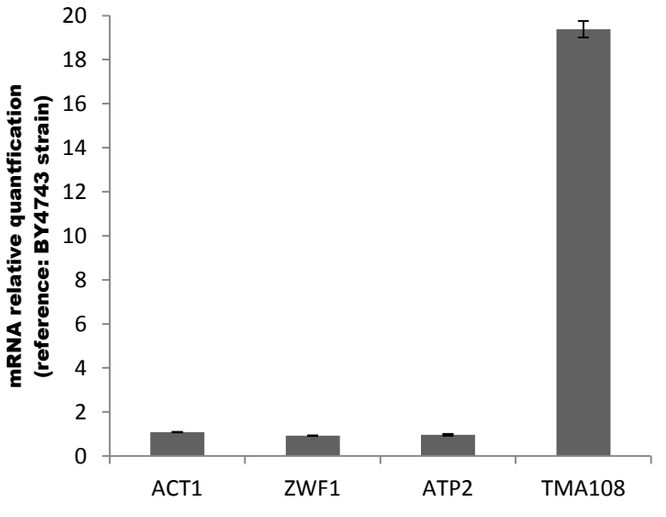
b
mRNA relative quantfication (reference: BY4743 strain)
ACT1
ZWF1
ATP2
TMA108

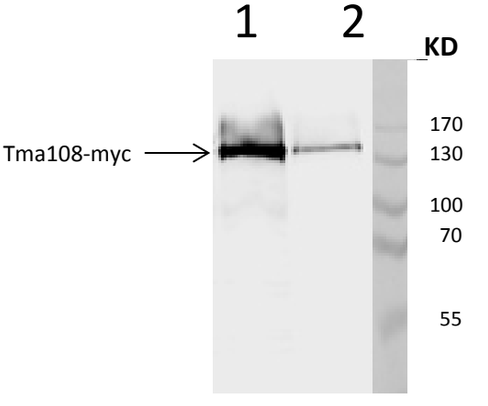
c
1
2
KD
Tma108-myc
170
130
100
70
55

Supplementary figure 7:

Tma108 recognize the N-terminal part of the nascent peptide: control and additional experiments

(a) Real-time quantitative RT-PCR analyses of the enrichment in Tma108-PA IPs of various ATP2 versions fused with a 300pb LacZ-derived Tag (construct 1'-3', see, Garcia et al. Embor, 2010). The arrows in bold indicate the positions of the primers used for the Q-PCR. The mean enrichment factor of two independent immunoprecipitation experiments corresponds to the ratio IP/Input normalized using ACT1 and ATP1 as control mRNAs. For each experiment, the enrichment of the endogenous ASN1 mRNA confirmed that Tma108-PA ribonucleoparticles were efficiently immunoprecipitated (data not shown).

(b) Real-time quantitative RT-PCR relative quantification of various ASN1 versions fused to a 13-myc Tag (construct 1-3). Ratios from two replicates are obtained following normalization to endogenous mRNA levels (ACT1, *ATP1* and *ASN1*).

(c) Input and immunoprecipitated fractions obtained from Tma108-PA (WT) and Tma108(MAMQN)-PA (mutant) cells were analysed by SDS page followed by western-blots using antibodies directed to the PA epitopes and Rpl1 and Rpl3 proteins.

(d) Input and immunoprecipitated fractions obtained from Tma108-PA expressing-cells transformed by plasmids allowing the expression of various ASN1 versions fused to a 13-myc Tag (construct 1-3 represented in figure S7b) were analyzed by SDS-PAGE followed by western-blots using antibodies directed to the Myc-tag and the PA epitopes.

a

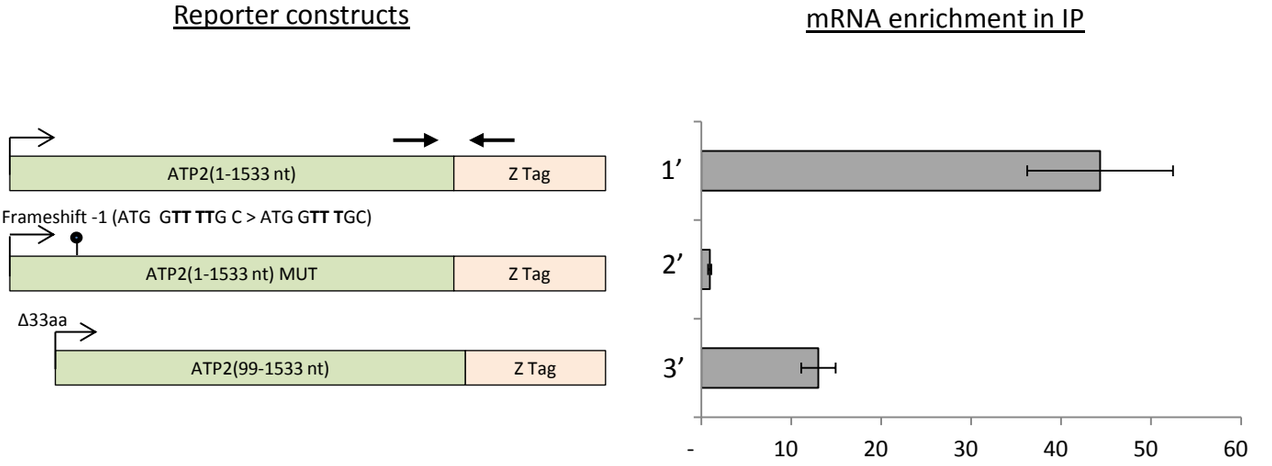
Reporter constructs
mRNA enrichment in IP
ATP2(1-1533 nt)
Z Tag
Frameshift -1 (ATG GTT TTG C > ATG GTT TGC)
ATP2(1-1533 nt) MUT
Z Tag
Δ33aa
ATP2(99-1533 nt)
Z Tag
1'
2'
3'
-
10
20
30
40
50
60

b

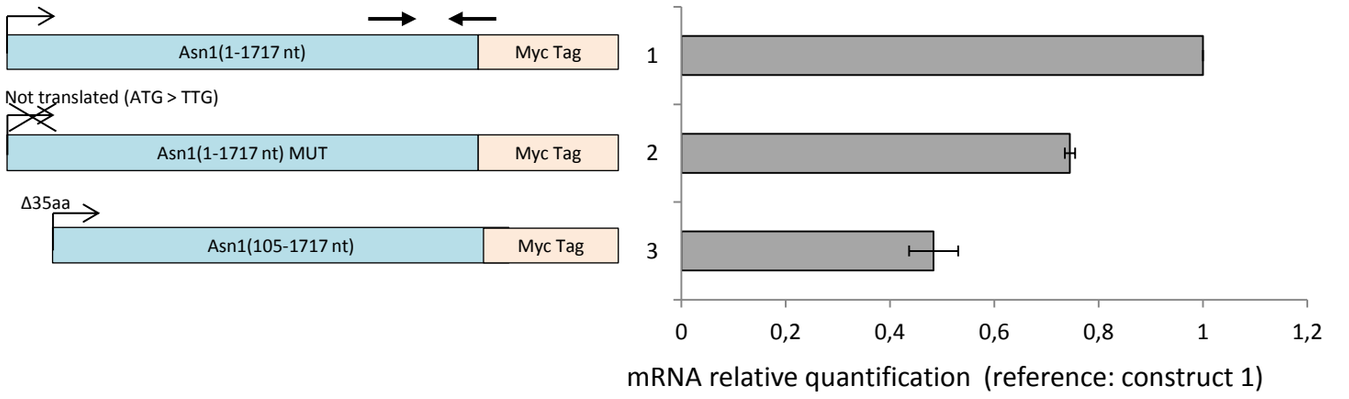
Asn1(1-1717 nt)
Myc Tag
Not translated (ATG > TTG)
Asn1(1-1717 nt) MUT
Myc Tag
Δ35aa
Asn1(105-1717 nt)
Myc Tag
1
2
3
0
0,2
0,4
0,6
0,8
1
1,2
mRNA relative quantification (reference: construct 1)

c

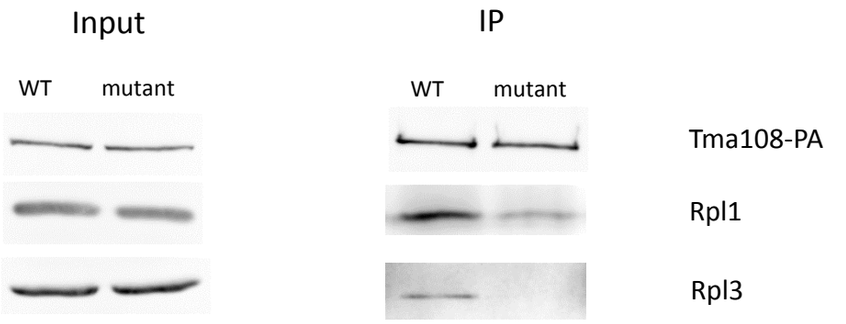
Input
IP
WT
mutant
WT
mutant
Tma108-PA
Rpl1
Rpl3

d

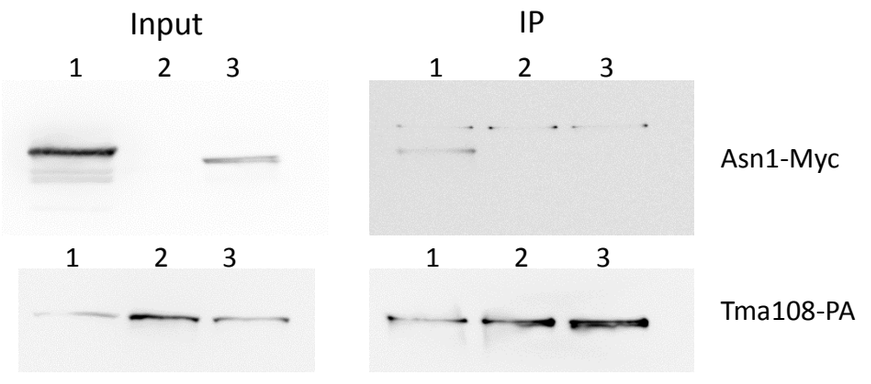
Input
IP
1
2
3
1
2
3
Asn1-Myc
1
2
3
1
2
3
Tma108-PA

Supplementary figure 8:

Tma108 deletion does not impact the steady state level of the global proteome

Comparative quantitative analysis of the proteome of BY4743 and TMA108 deleted strain. The log2 fold changes in protein abundances in TMA108(Δ/Δ) relative to BY4743 are plotted by the average normalized protein abundances. The proteins encoded by the target mRNAs of Tma108 are colored in blue. The quantification of protein abundances was performed using label free quantitative proteomics. Protein extracts were analyzed using Thermo Fisher instruments (San Jose, CA) available at the proteomics platform at the IJM http://www.ijm.fr/en/facilities/mass-spectrometry/, *i.e.* a LTQ Velos Orbitrap equipped with an EASY-Spray nanoelectrospray ion source, coupled to an Easy nano-LC Proxeon 1000 system. Label free quantitative proteomics was performed as described in (Léger et al., Methods Mol Biol. 2016, 1361:289-307). Two technical replicates were combined with two independent biological replicates, in order to obtain reproducible protein abundances in WT and ΔTMA108 strains. Among the proteins for which abundance values were available, those displaying significantly different levels between ΔTMA108 and WT strain were identified using the LIMMA program (Ritchie et al., Nucleic Acids Res. 2015, 43(7)). Only a few number of proteins exhibited significant changes meaning that the global proteome steady state level is not affected by Tma108 deletion.

Delaveau et al. Fig. S8